Skull Stripping for Improved Brain Tumor Detection In Orthogonal MRI Scans

Hend Fat'hy Khalil*
Modern Academy for Engineering and Technology, Cairo, Egypt.
Ashraf Mahroos Said†
Faculty of Engineering, Banha University, Banha, Egypt.
Hesham F. A. Hamed ‡
Minia University, Minia, Egypt.
Eman Mohammed Mahmoud §
Modern Academy for Engineering and Technology, Cairo, Egypt.

Abstract

Detecting brain tumors at an early stage is an incredibly demanding responsibility for radiologists. The rapid rate at which these tumors grow is deeply concerning. When left untreated, patients commonly experience a significantly lower survival rate, intensifying the situation to a critical and potentially life-threatening condition. Consequently, the urgent need arises for an automated system capable of early detection of brain tumors. In this research, we present an approach that offers a streamlined method to effectively distinguish between cancerous and non-cancerous brain Magnetic Resonance Imaging (MRI) scans across multiple planes, including the Axial, Coronal, and Sagittal planes. The methodology encompasses several distinct stages for lesion analysis, beginning with preprocessing techniques to eliminate noise and improve image quality. Next, K-means segmentation is employed to accurately segment cancerous cells from the surrounding tissue. Feature extraction is performed using various methods such as Discrete Wavelet Transform (DWT), Gray Level Co-occurrence Matrix (GLCM), and Principal Component Analysis (PCA) to extract informative features from the segmented regions. In the final step, a Support Vector Machine (SVM) classifier is employed to classify the extracted features and make predictions using the given dataset. The research study utilizes three SVM classifier tools, namely Linear, Gaussian, Polynomial SVM, for the proposed analysis. The proposed methodology consists of two distinct phases: the Skull Stripping phase and the non-skull stripping phase. Additionally, we proposed a method for accurately detecting the skull in MRI scans. It has been observed that by excluding the skull from the analysis, the accuracy of tumor detection improves by approximately 7% compared to when the skull is not removed from the scan. By leveraging automatic detection techniques; we facilitate the detection of tumors in any plane of MRI imaging. This approach offers a convenient and efficient method for identifying and localizing tumors across various imaging planes.

Key Words: Brain tumors, K-mean, SVM, MRI imaging.

1 Introduction

A brain tumor refers to an abnormal growth of cells in the brain or the central nervous system. There are two primary categories of brain tumors: primary and secondary. Primary brain tumors originate from the cells that constitute the brain and its surrounding tissues. In contrast, secondary brain tumors are tumors that have spread or metastasized from other parts of the body to the brain.

There are two types of brain tumors: benign and malignant. Malignant tumors can grow quickly and may spread to other parts of the body or brain, but benign tumors are usually non-cancerous and grow more slowly[1]. Different types of tumors are classified based on the specific cells involved.

Glioma brain tumors are a type of tumor that develops from glial cells in the brain. They can be either benign or malignant, with malignant gliomas being particularly dangerous. These tumors pose significant risks due to their location within the brain and their potential to invade surrounding healthy tissue[2]. The dangers associated with glioma brain tumors stem from their ability to disrupt vital brain functions and exert pressure on adjacent structures. As they grow, they can cause a range of neurological symptoms, including headaches, seizures, cognitive impairments, and changes in personality or behavior. The invasive nature of malignant gliomas makes complete surgical removal challenging, and they can also spread to other parts of the brain or spinal cord[3]. Treatment options can be limited, as gliomas may be resistant to certain therapies. Early detection of glioma is vital for initiating timely treatment, improving treatment outcomes, implementing appropriate surveillance, and empowering patients in their healthcare decisions[4].

*Communication and Electronics Department, Modern Academy for Engineering and Technology, Cairo, Egypt. Email:eng.hend2025@gmail.com.
†Biomedical Departments, Faculty of Engineering, Banha University, Banha, Egypt. Email: ashraf.mahrous@bhit.bu.edu.eg .
‡Faculty of Engineering, Minia University, Minia, Egypt. Email: hfah66@yahoo.com.
§1Communication and Electronics Department, Modern Academy for Engineering and Technology, Cairo, Egypt. Email: dremanmm@gamil.com.

Medical professionals utilize various imaging techniques to detect and diagnose brain tumors. Among these techniques, MRIs, or magnetic resonance imaging, are the most often used modality. MRI creates precise images of the brain using strong magnets and radio waves, making it possible to identify the features, size, and location of tumors[5]. Contrarily, computed tomography (CT) scans employ X-rays to produce cross-sectional brain pictures, which help evaluate tumor characteristics as well as any concomitant brain hemorrhage or edema[6].

MRI offers superior soft tissue contrast compared to CT scans, making it particularly effective in differentiating between different types of tissues[7]. It provides highly detailed and multi-planar images, enabling better visualization of brain tumors and the surrounding structures. To facilitate the interpretation and analysis of brain images, different imaging planes or orientations are commonly used.

The three orthogonal primary MRI brain planes employed in clinical practice and research are the axial plane, sagittal plane, and coronal plane. The axial plane, parallel to the ground when a person is upright, provides a comprehensive top-down view of the brain, allowing for assessment of structures like the cerebral hemispheres, ventricles, basal ganglia, thalamus, and brainstem. The sagittal plane divides the brain into left and right halves and offers a side view, revealing information about the cerebral cortex, corpus callosum, cerebellum, and midline structures[8]. Lastly, the coronal plane divides the brain into anterior and posterior sections, providing a frontal view that aids in assessing the frontal lobes, lateral ventricles, hippocampus, and other critical structures.

The three planes of MRI brain imaging, axial, sagittal, and coronal, each offer distinct anatomical perspectives, allowing for the identification and characterization of different brain regions, lesions, and abnormalities. By examining the brain in these orthogonal planes, radiologists and clinicians can gain valuable insights into the precise location, extent, and nature of brain pathologies. This comprehensive evaluation enables accurate diagnosis and effective treatment planning for patients. Figure (1) shows MRI brain images in multiple planes.

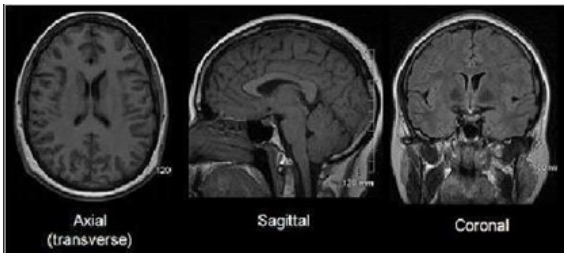

Figure 1: The descriptive process flow followed in the model

The proposed methodology comprises several sequential steps to facilitate the detection of tumors in any plane of MRI imaging, initiating with preprocessing methods to enhance image quality. Subsequently, K-means segmentation is applied to precisely delineate cancerous cells from the neighboring tissue. Then, extract meaningful features from the segmented regions. Finally, a Support Vector Machine (SVM) classifier is employed to classify the extracted features on the provided dataset. That experiment was implemented using MATLAB R2021a. The primary contributions of this research are as follows:

Automated Brain Tumor Detection and Classification: This study introduces an automated method aimed at detecting and classifying brain tumors using three orthogonal planes of MRI images. The proposed methodology encompasses multiple procedural stages, notably preprocessing, feature extraction, and classification.

Innovative Preprocessing Techniques: A novel skull stripping method is employed during the preprocessing phase, significantly impacting the accuracy of subsequent classification outcomes. This step plays a pivotal role in refining the input data for enhanced analysis.

Advanced Feature Extraction: In the feature extraction phase, a fusion of distinctive features is utilized, including:

- Tumor area feature
- Discrete Wavelet Transform (DWT) combined with Principal Component Analysis (PCA)
- Gray Level Co-occurrence Matrix (GLCM) features

These features encapsulate crucial tumor characteristics essential for classification.

Classification Strategy: The geometric family of Support Vector Machines (SVM) is employed, with various kernels such as Linear, Gaussian, and Polynomial, to determine the optimal configuration. This iterative process ensures the selection of the most effective classification approach.

Performance Evaluation on Kaggle Datasets: The proposed method undergoes rigorous evaluation using Kaggle datasets, with performance metrics primarily focusing on Accuracy (ACC).

2 Related Work

(Padlia, M., and Sharma, J. 2017) [9] Presents a technique for using T1-weighted and fluid- attenuated inversion recovery (FLAIR) brain images to identify and separate brain malignancies. A fractional Sobel filter is applied to the brain image to reduce noise and enhance its texture. The Sobel filter's fractional order () provides more versatility in optimizing the segmentation results. The detection of asymmetry between hemispheres is achieved through the application of Bhattacharya coefficients and mutual information. The hemisphere containing the tumor is determined using a histogram asymmetry method. Support vector machines (SVMs) are used to compute and classify statistical aspects of a specific window in order to segment the tumor region inside the recognized hemisphere. Images from the BRATS-2013 dataset are used for simulations, and performance measures like

specificity, sensitivity, and accuracy are calculated for various values. The outcomes of the simulation show that the suggested strategy outperforms the majority of similar current techniques.

(Kumar, Rashmi, Ramadoss, Sandhya, and Sangeetha 2017)[10] Present a Support Vector Machine (SVM) classifier-based approach for brain tumor detection. It starts with the acquisition of magnetic resonance imaging (MRI) brain scans, which provide detailed anatomical information for tumor detection. The MRI scans are preprocessed to enhance the quality of the images. Feature extraction is then performed on the preprocessed images. Features such as intensity, texture, and shape characteristics are computed from the tumor region. An SVM classifier is trained using the retrieved features as input. The SVM is a machine learning algorithm that learns to classify different patterns based on labeled training data. In MRI scans, the SVM classifier performs admirably in differentiating between tumor and non-tumor regions.

(Vani, N., Sowmya, A., & Jayamma, N. 2017) [11]develop a model that will help identify and categorize brain tumors. Specifically, the objective is to classify whether a tumor is cancerous or non-cancerous by utilizing the SVM algorithm. While Artificial Neural Networks (ANN) based on Empirical Risk Minimization has been used in prior studies for detection, this paper introduces the application of the Support Vector Machine algorithm, which operates on structural risk minimization, for image classification. The SVM algorithm is implemented on medical images to extract tumors, and a Simulink model is created for the purpose of tumor classification. In order to classify the images and determine whether they are malignant or not, the research presents a prototype for SVM-based object detection. This study maintains a high detection accuracy of 82

(Rashid, M. H. O., Mamun, M. A., Hossain, M. A., and Uddin, M. P. 2018)[12] Proposed a method that involved three main steps: anisotropic filtering, support vector machine (SVM) classification, and morphological operations. Anisotropic filtering was applied to enhance the MR images and improve the quality of the tumor region. This filtering technique selectively smoothes the image in different directions, preserving edges and details. After the anisotropic filtering, The tumor and non-tumor areas were classified using the SVM classifier. The ideal hyper plane that divides the data points into distinct classes is found via SVM. In the final step, morphological operations were performed on the classified image to refine the tumor region and remove any noise or artifacts. Morphological operations involve the manipulation of image pixels based on their spatial arrangement. According on the experimental results, the SVM achieved 83% segmentation accuracy.

(Birare and Chakkarwar. 2018) [13]develop an automated system that uses the support vector machine (SVM) algorithm to identify brain tumor cells. Manual detection of tumor cells in microscopic images is a time-consuming and error-prone process, hence the need for an automated system. The authors propose a methodology that involves multiple steps. Firstly, they acquire microscopic images of brain tumor cells. Then, they preprocess the images to enhance the features and remove any noise. Next, they extract relevant features from the preprocessed images, which serve as input to the SVM classifier. SVM was used in the experiment to identify malignant and normal cells with 98.51% accuracy.

(Selvapandian and Manivannan 2018) [14]addresses the challenging task of detecting tumor regions in Glioma brain images, which are often characterized by low sensitivity in boundary pixels. The Non-Subsampled Contourlet Transform (NSCT) is used to improve the brain image, and texture characteristics are then extracted from the improved image. The Adaptive Neuro Fuzzy Inference System (ANFIS) technique is then used to train and classify these extracted features, allowing it to discriminate between brain scans with gliomas and normal ones. Then, using morphological functions, the tumor regions in the Glioma brain picture are segmented. The performance of the proposed Glioma brain tumor detection algorithm is assessed on the publicly available Brain Tumor Image Segmentation Challenge (BRATS) dataset. The suggested approach achieves 96.7% accuracy.

(Keerthana and Xavier 2018) [15]introduce an intelligent system that seeks to identify and categorize brain cancers in their early stages. The system incorporates various stages, starting with image acquisition using magnetic resonance imaging (MRI). After image acquisition, Preprocessing methods are used to improve the MRI image quality. These methods could include noise removal, intensity normalization, and spatial filtering. Next, To extract valuable information from the preprocessed images, feature extraction is done. Statistics pertaining to texture, shape, and intensity are calculated based on the tumor region. Tumor categorization uses the support vector machine (SVM). The results demonstrate that the proposed intelligent system achieves high accuracy in the early assessment and classification of brain tumors.

(Amin, J., Sharif, M., Raza, M., Saba, T., and Anjum, M. A. 2019) [16]develop a method for brain tumor detection using a combination of statistical and machine learning techniques. The researchers proposed a framework that utilized statistical features extracted from brain images and employed machine learning algorithms for tumor detection. Magnetic resonance imaging (MRI) scans were primarily used as the imaging modality for brain tumor detection. The framework comprised several steps. Firstly, pre-processing techniques were applied to remove noise or artifacts and improve the quality of the MRI images. Subsequently, pertinent information on the tumor site was retrieved from the pre-processed images using statistical features like mean, standard deviation, skewness, and kurtosis. Various classifiers, include k-nearest neighbors (KNN), support vector machines (SVM), and decision trees were experimented with to determine the most effective approach for tumor classification. At the fused feature-based level, the obtained results showed a specificity of 1.00, sensitivity of 0.92, accuracy of 0.93, 0.96 for both the dice similarity coefficient (DSC) and area under the curve (AUC).

(Hussain and Khunteta 2020)[17]utilizes a set of MRI images

as input data and employs a series of preprocessing steps, including median filtering and skull stripping, to enhance the images. The thresholding process is performed using the watershed segmentation method to isolate the brain tumor tissues. After that, the gray-level co-occurrence matrix (GLCM) approach is used to extract features. A support vector machine (SVM) is then used to classify the images based on the features that were extracted. The system's accuracy on average is 93.05% surpassing the performance of other conventional models.

(Sharath Chander, Soundarya, and Priyadharsini 2020) [18]proposed method utilizes well-defined algorithms to handle challenging scenarios, such as poor image quality.To extract relevant tumor locations from the MRI data, an adaptive k-means clustering segmentation algorithm is used. The segmented images are then classified using a Support Vector Machine (SVM) classifier, which also helps identify the type of tumor. The linear kernel provides better accuracy results when the study compares the various SVM classifier kernel functions. By utilizing MRI imaging data, the proposed system seeks to offer a more precise method for brain tumor diagnosis and categorization.

(Chen et al. 2021) [19] provide a novel method for the automatic detection and classification of brain cancers utilizing support vector machines (SVMs) and extended Kalman filters (EKF). There were five parts to the EKF-SVM algorithm. The images were first subjected to image normalization, noise reduction using a non-local means filter, and contrast enhancement using enhanced dynamic histogram equalization. Second, image features were extracted using a gray- level co-occurrence matrix. Thirdly, an EKF was utilized to categorize brain cancers in the brain MRIs after the retrieved characteristics were supplied into an SVM to classify the MRI images initially. Fourth, cross-validation was done to confirm the classifier's accuracy. Lastly, brain tumors were identified using an artificial segmentation technique that included region growth and k-means clustering. The outcomes demonstrated that the EKF-SVM algorithm successfully classified brain tumors automatically with an astounding 96.05% accuracy rate.

(Shahajad, Gambhir, and Gandhi 2021) [20]proposes a method to determine the optimal number of quantifiable gray level co-occurrence matrix (GLCM) texture features for identifying brain cancers in medical MRI image collections as aberrant versus normal. After extracting all of the GLCM texture features from the MRI pictures, the best features are chosen via a method based on heat maps. The support vector machine (SVM) classifier then uses these chosen characteristics as input. Results show that the SVM classifier achieves high accuracy, with a peak testing accuracy of approximately 92% when using 6-7 features. However, further increasing the number of features does not lead to improved accuracy, as the accuracy plateaus.

3 Proposed Methodology:

Figure (2) Show the block diagram of proposed methodology.

3.1 MRI Scan of obtained Brain Tumor Images:

Magnetic Resonance Imaging (MRI) is a type of image that is represented using 8 bits, containing brightness information ranging from 0 to 255. A pixel value of '0' in this notation denotes black color, and a value of '255' denotes white color. We resized the MRI images to dimensions of 200x200 pixels. Grayscale images, which only consist of brightness information and lack color information, were used in this specific case.

3.2 Preprocessing:

3.2.1 Vertical Flipping for Sagittal plane images:

In the case of sagittal images, it is important to consider the different directions, namely right and left. When these images are utilized with varying directions, it can lead to a decrease in accuracy. To mitigate this issue, a possible solution is to flip all the images in the right direction. By consistently using a single direction, it has been observed that accuracy tends to increase.

3.2.2 3.2.2. Detected Area of tumor:

In this study, we proposed approach for the identification and quantification of tumor regions within medical images. Our method encompasses several stages, starting with the conversion of the original image into a binary representation. Subsequently, we proceed to calculate the solidity and area metrics for the detected regions. By comparing the density of these regions against a predefined threshold (0.5), we select the region with the highest density as the primary area of interest. To enhance the discriminatory power of our analysis, we employ advanced techniques for feature extraction. Specifically, we utilize the extracted area of the tumor region as a fundamental feature, which is then combined with features derived from Principal Component Analysis (PCA) and Gray-Level Co-occurrence Matrix (GLCM). This fusion of features allows for a comprehensive and multidimensional representation of the tumor, enabling a more refined and scientifically grounded analysis. Through the integration of these innovative methodologies, our research offers a robust and sophisticated framework for tumor area detection. By leveraging binary image conversion, density-based selection, and feature fusion techniques, we have achieved a significant advancement in the identification and characterization of tumor regions in medical imaging, paving the way for improved diagnostic accuracy and treatment planning.

3.2.3 3.2.2. Median Filter:

A nonlinear filter is the median filter. It operates extremely effectively to eliminate the "salt and pepper" noise, or impulse noise, from the image. The rationale behind the median filter

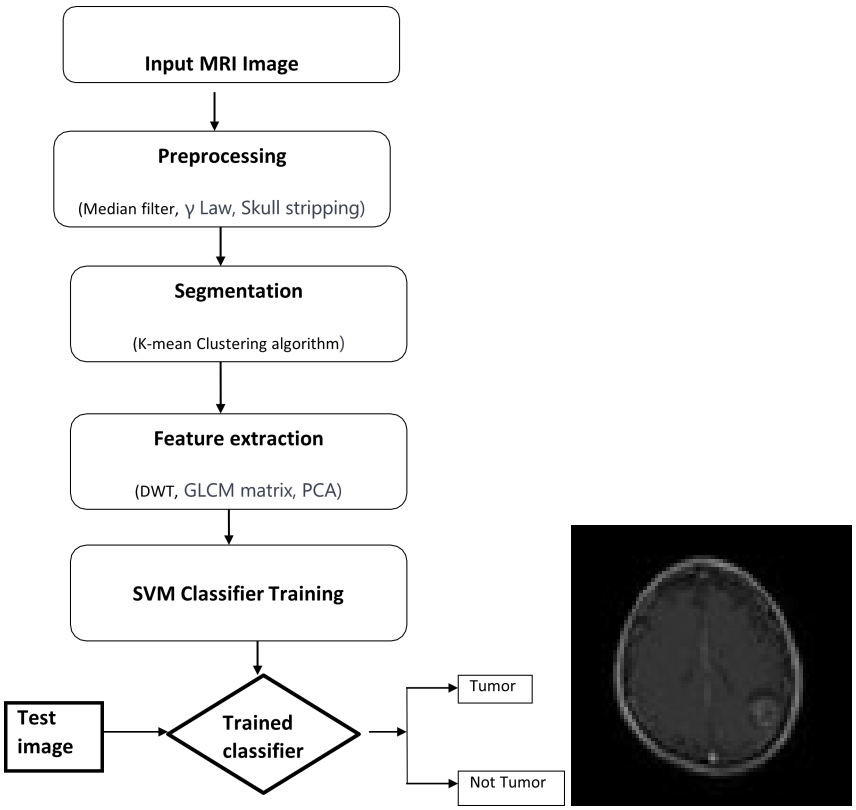

is to use the median of the gray levels in a neighborhood surrounding each pixel to replace the gray level of each individual pixel.

The following is a definition of the median filter operation:

$$I'(x,y) = \text{median}\,(I(x+i,y+j)) \quad \text{for} \quad (i,j) \in \text{filter window}$$

Where: I represents input image, I' represents the filtered image, (x, y) represents the pixel position in the image, and (x+i, y+j) represents the neighboring pixels within the filter window centered at (x, y). The filter window size is usually odd to ensure there is a unique median value. The median function sorts the pixel values within the window and selects the middle value as the new pixel value. The median is determined by averaging the two middle values if the number of pixels in the window is even.

3.2.4 Gamma Law:

For many image processing applications, such as color correction, image enhancement, and display calibration, gamma correction is a necessary first step. Gamma correction is a method that modifies an image's brightness or contrast by transforming the pixel values non-linearly. In the context of image preprocessing, gamma correction is often applied to compensate for the non-linear relationship between pixel values and perceived brightness. The gamma correction function is typically expressed as:

$$V\_\text{out} = V\_\text{in}^{\gamma} \tag{2}$$

Where:

- V_{out} is the corrected pixel value after gamma correction
- V_{in} is the original pixel value
- γ is the gamma parameter that controls the intensity transformation

The gamma parameter γ determines the degree of correction applied to the image. If $\gamma < 1$, the image becomes brighter because the transformation amplifies the lower pixel values. On the other hand, if $\gamma > 1$, the image becomes darker as the transformation compresses the lower pixel values[21].

3.2.5 Skull Stripping:

Skull stripping, also known as brain extraction or skull removal, is a process in medical image analysis that involves segmenting the brain tissue from other structures such as the skull and scalp in neuroimaging data, usually from scans using magnetic resonance imaging (MRI). There are various methods used for skull stripping in MRI images such as Thresholding, Region growing, and Cropping.

In this research, we introduce a precise methodology for the identification and subsequent removal of the skull from MRI images. Firstly, we employ a binary image conversion technique and conduct connected component analysis on the MRI data. Subsequently, we assess the solidity area and employ a condition wherein if this area falls below a predetermined threshold value, it is deemed skull-free; conversely, if the

solidity area exceeds the threshold value, it is identified as the presence of the skull.

Secondly, we employ the Sobel edge detection algorithm to discern the edges of the skull accurately. Following this, we normalize the MRI image and perform subtraction of the detected skull from it, resulting in a refined image without the skull artifact.

By employing these scientific methodologies, we achieve a precise and reliable means of skull detection and removal from MRI images. Figure (3) represents the block diagram of Skull Stripping methodology.

3.3 Segmentation:

3.3.1 K-Mean Clustering:

Then update by making Recalculate the cluster centers μ_i based on the pixels assigned to each cluster according to this equation:

$$\mu_i = \frac{1}{|C_i|} \sum_{p \in C_i} p$$

where C_i represents the set of pixels assigned to cluster i, and $|C_i|$ is the number of pixels in that cluster. This process of assignment and update is repeated iteratively until convergence, where the cluster centers do not significantly change between iterations.

3.4 Feature Extraction:

3.4.1 Discrete Wavelet Transform (DWT):

An analytical mathematical method for signal processing and data analysis is the Discrete Wavelet Transform. It breaks down a signal into its constituent frequency components so that it can be analyzed on various scales[**?**]. The DWT is based on wavelets, which are small waveforms or functions that are scaled and shifted to analyze different parts of a signal. The signal is transformed by running it through a number of filters that divide it into several frequency ranges. Mathematically, the DWT can be represented by the following equation:

$$\mathrm{DWT}(x) = \sum_k h_k \cdot (x * \phi_k) + \sum_j \sum_k g_k \cdot (x * \psi_{jk})$$

Where, x represents the input signal, ϕ_k and ψ_{jk} are the scaling and wavelet functions, respectively. The coefficients h_k and g_k are the filter coefficients associated with the scaling and wavelet functions. The symbol $*$ denotes the convolution operation. By performing the DWT, the original signal can be decomposed into different frequency bands, often referred to as approximation and detail coefficients[**?**]. The high-frequency details are captured by the detail coefficients, whilst the low-frequency components are represented by the approximation coefficients.

3.4.2 Principal Component Analysis PCA:

PCA, or Principal Component Analysis, is a statistical technique that simplifies and visualizes high- dimensional data. The method accomplishes this by locating the principal components, which are linear combinations of the initial variables that account for the majority of the variance in the observations[25]. Mathematically, PCA involves several steps. The data is first normalized by dividing by the standard deviation and subtracting the mean. Next, a covariance matrix is computed to capture the relationships between variables. The eigenvectors and eigenvalues of the covariance matrix are then calculated through an eigendecomposition. The eigenvectors represent the principal components, while the eigenvalues indicate the amount of variance each component explains. By selecting the top k eigenvectors with the highest eigenvalues, a reduced-dimensional space is formed. Finally, the data is transformed by multiplying the standardized data matrix with the matrix formed from the selected principal components. The most important patterns and information are preserved while the data can be visualized and analyzed in a lower-dimensional space due to this transformation[26].

Following the utilization of Principal Component Analysis (PCA) and the Discrete Wavelet Transform (DWT), we have extracted seven features, representing the most salient components of the data. These features have been derived using advanced mathematical techniques to capture essential patterns and information. The DWT has allowed for a multi resolution analysis of the data, decomposing it into different frequency bands. PCA then found the principle components that explain the largest variance, thereby reducing the dimensionality. We have derived a succinct collection of seven features (Mean, Standard deviation, RMS, Variance, Entropy, Smoothness, and Skewness) that capture the most important and scientifically meaningful aspects of the data through this combined technique.

Mean:

$$\text{Mean} = \frac{1}{N} \sum_{i=1}^{N} x_i$$

Standard Deviation:

$$\text{Standard Deviation} = \sqrt{\frac{1}{N} \sum_{i=1}^{N} (x_i - \text{mean})^2}$$

2. RMS (Root Mean Square):

$$\text{RMS} = \sqrt{\frac{1}{N} \sum_{i=1}^{N} x_i^2}$$

3. Variance:

$$\text{Variance} = \frac{1}{N} \sum_{i=1}^{N} (x_i - \text{mean})^2$$

4. Entropy:

$$\text{Entropy} = -\sum p(x) \cdot \log_2(p(x))$$

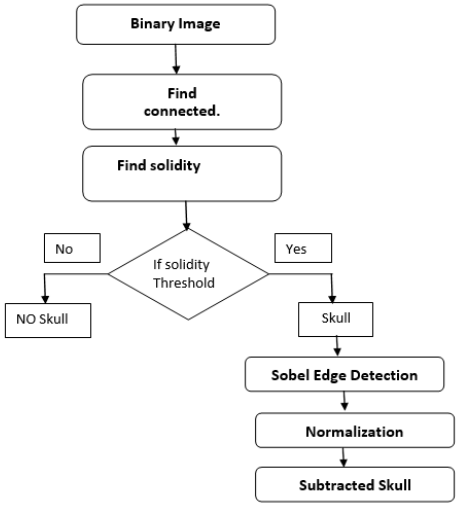

Figure 2: represents the block diagram of Skull Stripping methodology.

5. Smoothness:

$$\text{Smoothness} = \frac{1}{N}\sum_{i=1}^{N}(x_i - \mu)^2$$

6. Skewness:

$$\text{Skewness} = \frac{1}{N}\sum_{i=1}^{N}\frac{(x_i - \text{mean})^3}{\text{std\_dev}^3}$$

Where N is the total number of pixels in the image, Σx is the sum of pixel values, $\Sigma(x-\text{mean})^2$ is the total of squared discrepancies between each pixel value and the mean, Σx^2 is the sum of squared pixel values in the image, $p(x)$ is the probability of occurrence of each pixel value in the image, and the summation is performed over all possible pixel values, $\Sigma(x-\mu)^2$ is the sum of squared differences between each pixel value and the average of its neighboring pixels, $\Sigma\left(\frac{(x-\text{mean})^3}{\text{std\_dev}^3}\right)$ is the total of the cubed differences between each pixel value and the mean, divided by the cubed standard deviation.

3.4.3 Gray-Level Co-occurrence Matrix (GLCM):

A texture analysis method called the Gray-Level Co-occurrence Matrix (GLCM) is used to map out the spatial correlations between an image's pixel intensities. It provides information about the texture patterns present in an image by quantifying the co-occurrence of different pixel intensity values at specified pixel distances and angles. GLCM works by constructing a matrix that counts the frequency of occurrence of pairs of pixel values at a given distance and angle[17]. The GLCM matrix is typically square and symmetric, with each element representing the number of times a particular pair of pixel values appears in the specified spatial relationship. From the GLCM matrix, various statistical measures can be derived to describe different aspects of texture, such as contrast, correlation, energy, and homogeneity. These measures capture information about the distribution and spatial patterns of pixel values in an image, providing insights into the texture characteristics.

Contrast:
Calculates the difference in local intensity between adjacent pixels.

$$\text{Contrast} = \sum_{i,j}(i-j)^2 \cdot P(i,j)$$

Correlation:
Calculates the linear dependence between two pairs of pixels.

$$\text{Correlation} = \frac{\sum_{i,j}(i-\mu_i)(j-\mu_j)\cdot P(i,j)}{\sigma_i \cdot \sigma_j}$$

Energy (additionally referred to as Angular Second Moment):
Reflects the overall uniformity or homogeneity of the image.

$$\text{Energy} = \sum_{i,j}[P(i,j)]^2$$

Homogeneity:
Calculates the degree to which the GLCM diagonal and the element distribution are closest to one another.

$$\text{Homogeneity} = \sum_{i,j}\frac{P(i,j)}{1+|i-j|}$$

3.5 SVM Classifier:

SVM, or Support Vector Machine, is a powerful and widely used classification algorithm in machine learning. It looks for the best hyper plane in a high-dimensional feature space to divide various classes of data points. The primary goal of SVM is to maximize the margin, or the separation between

each class's closest data points and the hyper plane[27]. SVM facilitates improved robustness and generalization by optimizing the margin.

The linear SVM classifier is the basic form of SVM that uses a linear decision boundary. It assumes that the classes can be separated by a straight line or hyper plane. The equation of a linear SVM classifier can be represented as:

$$f(x) = \mathbf{w}^T \cdot \mathbf{x} + b$$

Where x is the input feature vector, w is the weight vector, b is the bias term, and f(x) is the decision function.

The Gaussian (RBF), polynomial, and other kernel-based SVM classifiers are extensions of the linear SVM that allow for non-linear decision boundaries[28]. In order to accomplish this, they convert the input data into a higher-dimensional space that allows for the establishment of a linear decision boundary. The mapping from the original feature space to the higher-dimensional space is determined by the kernel function. The following formula applies to the Gaussian (RBF) SVM classifier:

$$f(x) = \sum_i \alpha_i \cdot K(x_i, x) + b$$

Where $f(x)$ is the decision function, α_i are the support vector coefficients, x_i are the support vectors, K is the kernel function (typically the Gaussian or radial basis function), and b is the bias term.

Similarly, for the polynomial SVM classifier, the equation is:

$$f(x) = \sum_i \alpha_i \cdot (x_i^T \cdot x + c)^d + b$$

Where $f(x)$ is the decision function, d is the polynomial degree, b is the bias term, c is a constant term, and α_i and x_i are the support vector coefficients and support vectors, respectively.

These variations of SVM classifiers allow for more flexible decision boundaries, enabling them to wrestle with intricate and non-linear classification issues. The choice of the kernel function and its associated parameters can significantly impact the performance of the SVM classifier in different scenarios.

4 Experimental Result:

Dataset used:

The MRI images utilized in this study were obtained from the website (www.kaggle.com). Magnetic Resonance Imaging (MRI) scans were employed, capturing images across multiple planes with a resolution of 200*200 pixels in JPEG format. The implemented methodology was carried out using Matlab 2021a.

The proposed research has successfully completed the process of tumor region detection from A total of 171 axial, 150 sagittal, and 153 coronal brain MRI images. This detection was achieved through the utilization of operations for both skull stripping and non-skull stripping.

In the skull stripping phase, operations were applied to remove the skull and isolate the brain region. The brain tumor region was then located using the K-mean segmentation technique. In the non-skull stripping phase, the images were directly subjected to the K-mean segmentation technique to detect the tumor region without prior skull stripping.

Four GLCM features (contrast, correlation, energy, and homogeneity) were also computed for these images as part of the investigation.

Fusion of Extracted Features:

In our study, we employed feature fusion by combining the features extracted from three different sources: the Gray-Level Co-occurrence Matrix (GLCM), Principal Component Analysis (PCA), Discrete Wavelet Transform (DWT), and tumor area detection. A Support Vector Machine (SVM) classifier was trained using the combined features acquired from these various approaches.

The first set of features was derived from the tumor area detection, which involved identifying and analyzing the specific regions of interest related to tumors in the medical images. This allowed us to capture relevant information specific to the tumor characteristics. The second set of features came from applying DWT and PCA. A signal processing method called DWT divides the image into many frequency bands, while PCA reduces the dimensionality of the feature space by identifying the most significant components. By combining DWT and PCA, we were able to extract features that captured both the frequency-based and spatial variations within the image. The third set of features was obtained from GLCM analysis, which measures the spatial correlations between the image's pixel intensities. GLCM provides information about the texture patterns present in the image, and the derived features help characterize the texture properties.

By fusing these three sets of features, we aimed to capture complementary information from different aspects of the image data. This fusion approach allowed us to leverage the unique strengths of each feature extraction method and create a more comprehensive representation of the image content. Finally, the combined features were fed into an SVM classifier, a potent machine learning technique that is well-known for executing well on classification challenges. The SVM classifier utilized the extracted features to learn and build a decision boundary that could accurately classify new and unseen medical images into appropriate categories, aiding in medical diagnosis and decision-making processes. Figure (4) show the features fusion In the subsequent phase, the classification of images was performed using three types of Support Vector Machine (SVM) classifiers, namely linear, Gaussian, and polynomial classifiers. The images were categorized into two phases: the non-skull stripping phase and the skull stripping phase. The accuracy of each MRI image plane in these two phases was evaluated, and the outcomes for the linear classifier, Gaussian classifier, and polynomial classifier were shown in Tables 1 through 3. It was observed that skull stripping is a critical step in the classification process, as it led to a significant improvement in accuracy by approximately 7% compared to the non-stripping phase.

The largest connected (solid) volume is the main tumor

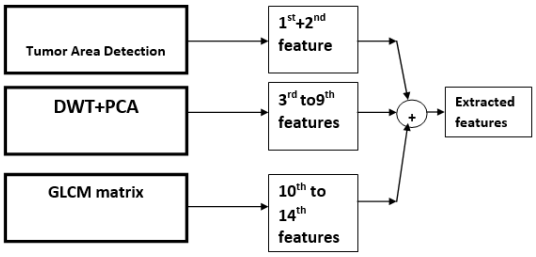

Figure 3: show the features fusion.

Table 1: Accuracy for Linear SVM Classifier

MRI Plane	NO. of Images	Without Skull Removal	With Skull Removal
Coronal	153	74.194%	88.71%
Axial	171	79.71%	86.957%
Unflipped Sagittal	150	64.912%	73.685%
Sagittal	150	75%	81.667%

Table 2: Accuracy for Gaussian SVM Classifier

MRI Plane	NO. of Images	Without Skull Removal	With Skull Removal
Coronal	153	75.807%	82.258%
Axial	171	75.362%	82.609%
Unflipped Sagittal	150	59.649%	64.912%
Sagittal	150	75%	78.333%

Table 3: Accuracy for Polynomial SVM Classifier

MRI Plane	NO. of Images	Without Skull Removal	With Skull Removal
Coronal	153	70.968%	82.258%
Axial	171	73.913%	79.71%
Unflipped Sagittal	150	56.14%	70.175%
Sagittal	150	65%	81.667%

volume. The training dataset was used to compute the distance from each smaller volume (secondary tumor volumes), which were calculated to the main tumor.

The findings for all 171 trained axial plane MRI images for the various linear, Gaussian, and polynomial classifiers are shown in Figure 5. The final classification is shown in 5(a),

where the support vectors classifier is represented by circle (o), the normal images are represented by blue dots, and the glioma (abnormal) tumor images are indicated by red dots. The mesh graph for deriving the least feasible point objective function model is shown in 5(b). The contour lines on the x-y plane show that the estimated goal function's accuracy has increased. The comparison between the next objective function value and the minimum objective function values is shown in 5(c).

The findings for all 153 trained Coronal plane MRI images for various linear, Gaussian, and polynomial classifiers are shown in Figure 6. The final classification is shown in 6(a), where the support vectors classifier is represented by circle (o), the normal images are represented by blue dots, and the glioma (abnormal) tumor images are indicated by red dots. The mesh graph for finding the least feasible point's objective function model is shown in 6(b). The contour lines on the x-y plane show that the estimated goal function's accuracy has increased. The comparison between the next objective function value and the minimum objective function values is shown in 6(c).

The findings for all 150 trained saggital plane MRI images for the various linear, Gaussian, and polynomial classifiers are shown in Figure 7. Final classification is shown in 7(a), where circle (o) denotes the support vector classifier, blue dots indicate normal images, and red dots indicate glioma (abnormal) tumor images. The mesh graph for deriving the least feasible point objective function model is shown in 7(b). The contour lines on the x-y plane show that the estimated goal function's accuracy has increased. The comparison between the next objective function value and the minimum objective function values is shown in 7(c).

The findings for all 150 trained unflipped saggital plane MRI images for the various linear, Gaussian, and polynomial classifiers are shown in Figure 8. The final classification is shown in

8(a), where the circle (o) denotes the support vector classifier, the blue dots indicate the normal images, and the red dots indicate the images of gliomas (abnormal tumors). The mesh graph for finding the least feasible point objective function model is given in 8(b). The contour lines on the x- y plane show that the estimated goal function's accuracy has increased. The comparison between the next objective function value and the minimum objective function values is shown in 8(c).

Figure 9(a) show original image,9(b) show the detected skull,9(c)show the image after skull stripping and 9(d) show the detected tumor for axial, coronal and saggital plane MRI images.

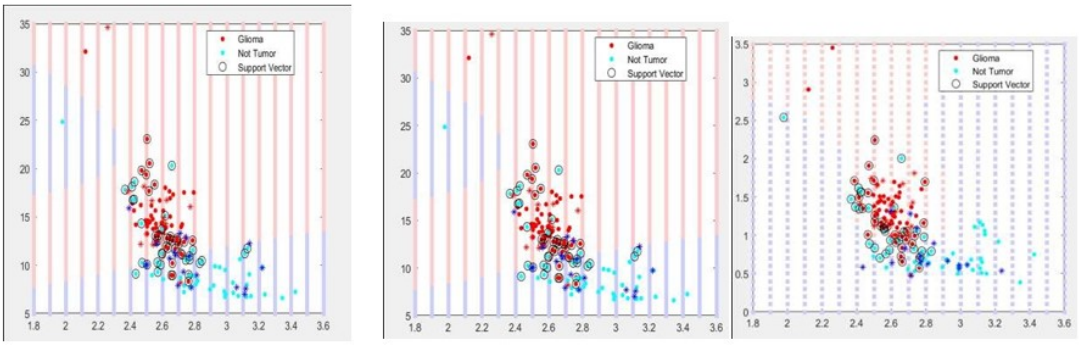

Figure 4: (a) Final classification

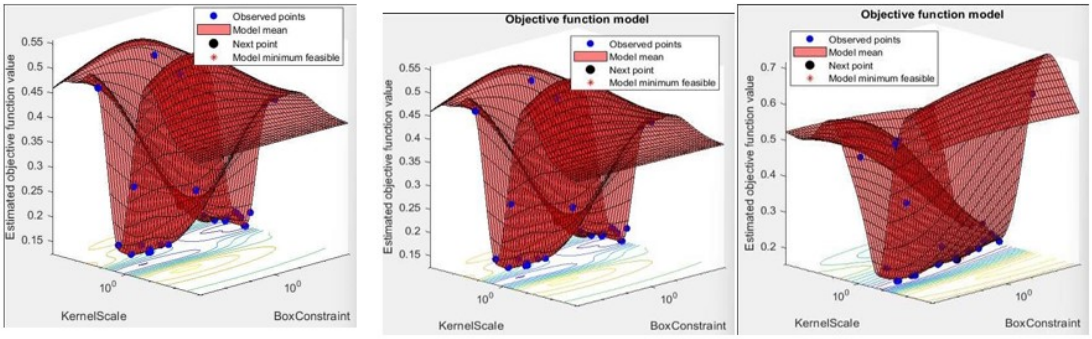

Figure 5: (b) Objective function

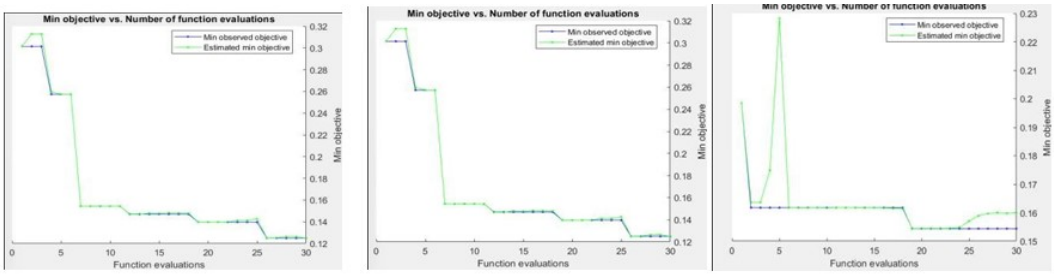

Figure 6: Comparison of Minimum Observed and Estimated Objective Values using Linear, Gaussian, and Polynomial Classifiers for SVM on Axial Plane MRI Image

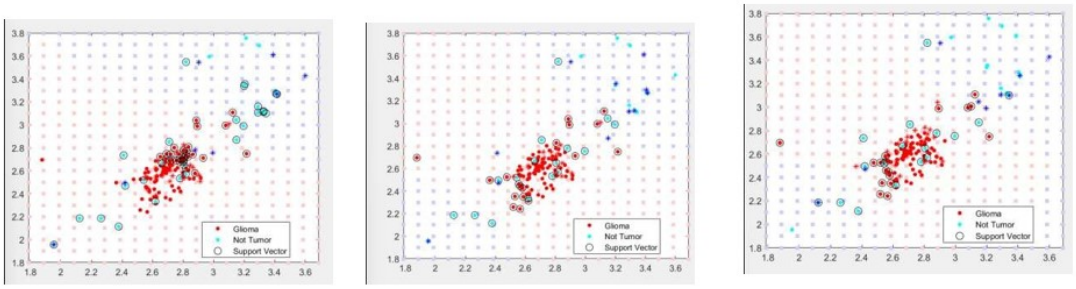

Figure 7: (a) Final classification

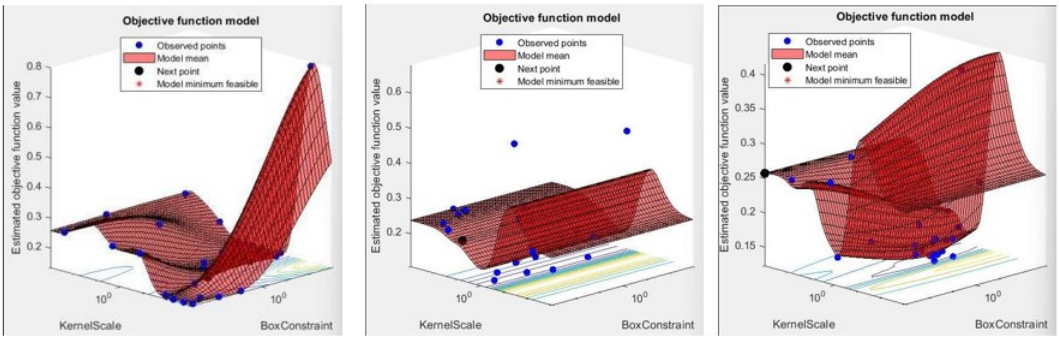

Figure 8: (b) Objective function

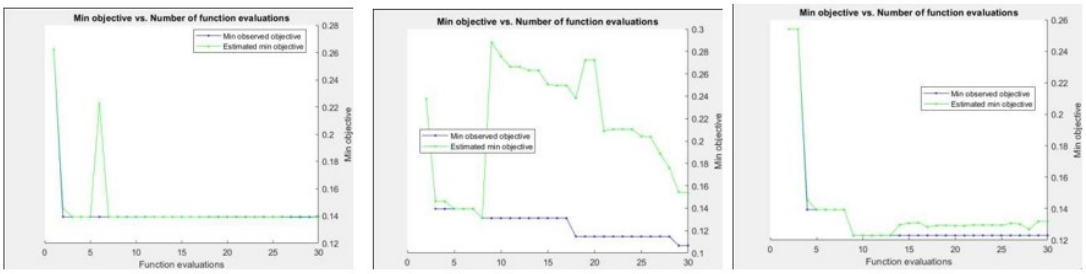

Figure 9: (b) Objective function:Linear Classifier: Gaussian Classifier:Polynomial Classifier: SVM for Coronal plane MRI image

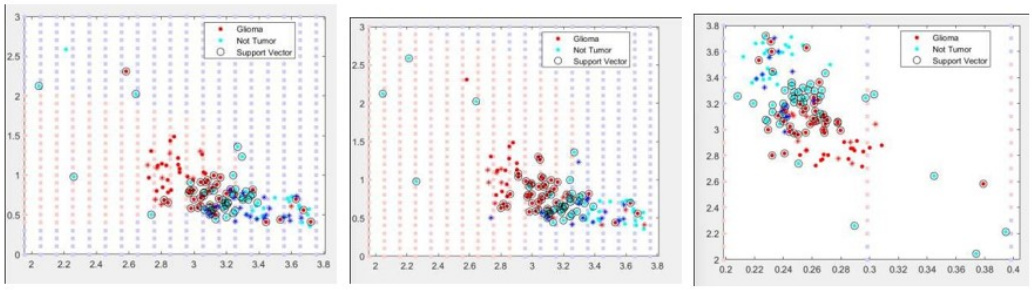

Figure 10: (a) Final classification

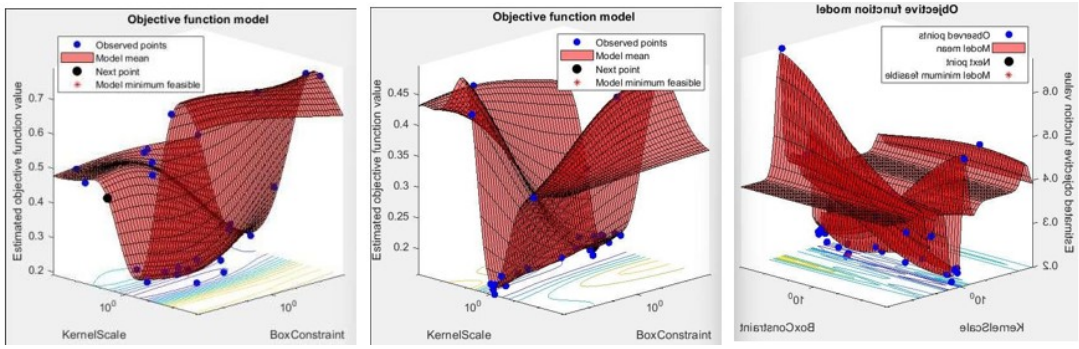

Figure 11: (b) Objective function

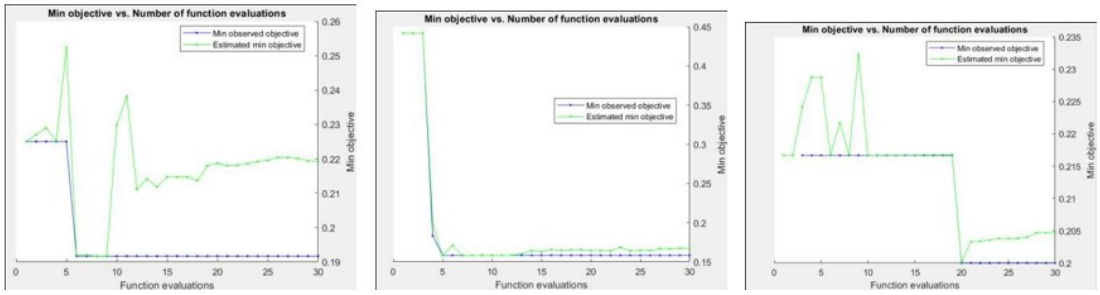

Figure 12: (c) Comparison of Min observed objective and estimated Min objective values Linear Classifier Gaussian Classifier Polynomial Classifier Figure 8: SVM for Unflipped saggital plane MRI image

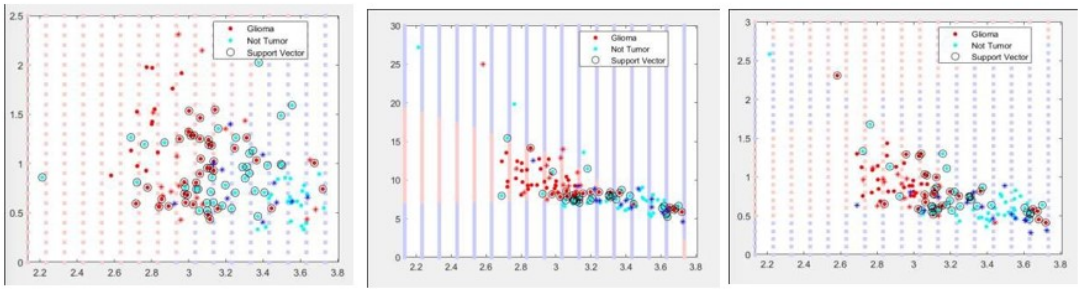

Figure 13: (a) Final classification

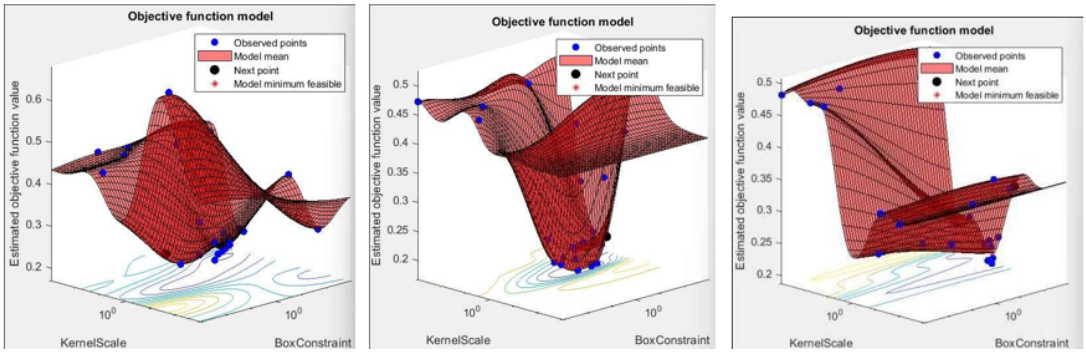

Figure 14: (b) Objective function

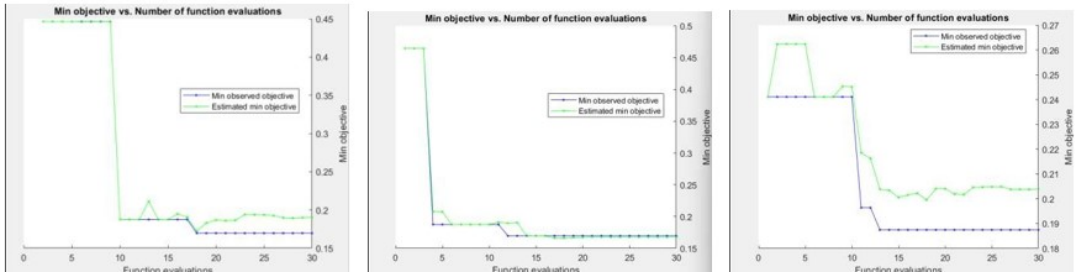

Figure 15: (c) Comparison of Min observed objective and estimated Min objective values Linear Classifier Gaussian Classifier Polynomial Classifier Figure 8: SVM for Unflipped saggital plane MRI image

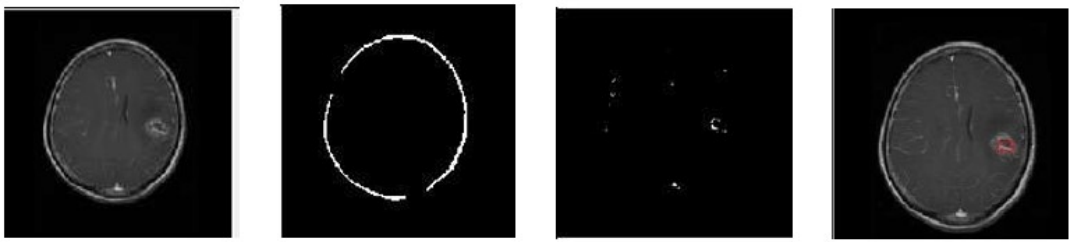

Figure 16: Axial Plane MRI Image (The original image)

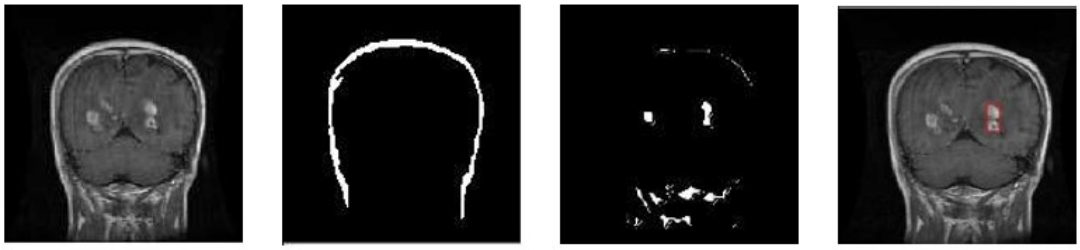

Figure 17: Coronal Plane MRI Image (The detected skull)

Figure 18: Sagittal Plane MRI Image (the image after skull stripping (d) the detected tumor)

5 Conclusion

This study presented a streamlined approach for accurately differentiating cancerous and non-cancerous brain MRI scans. The method involves preprocessing, K-means segmentation, and feature extraction using DWT, GLCM, and PCA. A SVM classifier is used for classification, and three SVM classifier tools are employed. The study also includes a skull detection method. Excluding the skull improves tumor detection accuracy by approximately 7%. The proposed approach enables tumor detection in all MRI imaging planes, providing a convenient and efficient method for tumor identification and localization.

References:

1 D. N. Louis et al., "The 2016 World Health Organization Classification of Tumors of the Central Nervous System: a summary," *Acta Neuropathol.*, vol. 131, no. 6, pp. 803–820, 2016, doi: 10.1007/s00401-016-1545-1.

2 M. Weller, W. Wick, M. E. Hegi, R. Stupp, and G. Tabatabai, "Should biomarkers be used to design personalized medicine for the treatment of glioblastoma?," *Futur. Oncol.*, vol. 6, no. 9, pp. 1407–1414, 2010, doi: 10.2217/fon.10.113.

3 Q. T. Ostrom et al., "CBTRUS statistical report: Primary brain and other central nervous system tumors diagnosed in the United States in 2009-2013," *Neuro. Oncol.*, vol. 18, pp. v1–v75, 2016, doi: 10.1093/neuonc/now207.

4 D. Chow, P. Chang, B. D. Weinberg, D. A. Bota, J. Grinband, and C. G. Filippi, "Imaging genetic heterogeneity in glioblastoma and other glial tumors: Review of current methods and future directions," *Am. J. Roentgenol.*, vol. 210, no. 1, pp. 30–38, 2018, doi: 10.2214/AJR.17.18754.

5 W. Reith, "Spinal column," *Diagnostic Interv. Radiol.*, vol. 22, no. March, pp. 269–350, 2016, doi: 10.1007/978-3-662-44037-7_10.

6 S. Hussain et al., "Modern Diagnostic Imaging Technique Applications and Risk Factors in the Medical Field: A Review," *Biomed Res. Int.*, vol. 2022, 2022, doi: 10.1155/2022/5164970.

7 S. Bhadani, S. Mitra, and S. Banerjee, "Fuzzy volumetric delineation of brain tumor and survival prediction," *Soft Comput.*, vol. 24, no. 17, pp. 13115–13134, 2020, doi: 10.1007/s00500-020-04728-8.

8 A. A. Mossa and U. Çevik, "Ensemble learning of multiview CNN models for survival time prediction of brain tumor patients using multimodal MRI scans," *Turkish J. Electr. Eng. Comput. Sci.*, vol. 29, no. 2, pp. 616–631, 2021, doi: 10.3906/ELK-2002-175.

9 V. Nath, Jyotsna, and K. Mandal, *Lecture Notes in Electrical Engineering 511 Nanoelectronics, Circuits and Communication Systems Proceeding of NCCS 2017*. 2017. [Online]. Available: `http://www.springer.com/series/7818`.

10 T. Sathies Kumar, K. Rashmi, S. Ramadoss, L. K. Sandhya, and T. J. Sangeetha, "Brain tumor detection using SVM classifier," *Proc. 2017 3rd IEEE Int. Conf. Sensing, Signal Process. Secur. ICSSS 2017*, pp. 318–323, 2017, doi: 10.1109/SSPS.2017.8071613.

11 U. S. Sudeep, K. N. Naidu, P. S. Girish, T. N. Nikesh, and C. Sunanda, "Brain Tumor Classification using a Support Vector Machine," *Int. J. Comput. Appl.*, vol. 184, no. 28, pp. 15–17, 2022, doi: 10.5120/ijca2022922347.

12 M. H. O. Rashid, M. A. Mamun, M. A. Hossain, and M. P. Uddin, "Brain Tumor Detection Using Anisotropic Filtering, SVM Classifier and Morphological Operation from MR Images," *Int. Conf. Comput. Commun. Chem. Mater. Electron. Eng. IC4ME2 2018*, pp. 3–6, 2018, doi: 10.1109/IC4ME2.2018.8465613.

13 G. Birare and V. A. Chakkarwar, "Automated Detection of Brain Tumor Cells Using Support Vector Machine," *2018 9th Int. Conf. Comput. Commun. Netw. Technol. ICCCNT 2018*, pp. 1–4, 2018, doi: 10.1109/ICCCNT.2018.8494133.

14 A. Selvapandian and K. Manivannan, "Fusion based Glioma brain tumor detection and segmentation using ANFIS classification," *Comput. Methods Programs Biomed.*, vol. 166, pp. 33–38, 2018, doi: 10.1016/j.cmpb.2018.09.006.

15 S. Jayapal, J. Jebathangam, K. Sharmila, and R. Bhuvana, "An intelligent system for early assessment and classification of brain tumor in MRI images using PNN," *Int. J. Sci. Technol. Res.*, vol. 9, no. 4, pp. 1563–1566, 2020.

16 J. Amin, M. Sharif, M. Raza, T. Saba, and M. A. Anjum, "Brain tumor detection using statistical and machine learning method," *Comput. Methods Programs Biomed.*, vol. 177, pp. 69–79, 2019, doi: 10.1016/j.cmpb.2019.05.015.

17 A. Hussain and A. Khunteta, "Semantic Segmentation of Brain Tumor from MRI Images and SVM Classification using GLCM Features," *Proc. 2nd Int. Conf. Inven. Res. Comput. Appl. ICIRCA 2020*, pp. 38–43, 2020, doi: 10.1109/ICIRCA48905.2020.9183385.

18 E. Chew, *In Love and War with Service Robots: The Passionate Deployment, Challenges and National Policy Implications*. 2020, doi: 10.1007/978-981-13-8323-6_30.

19 B. Chen, L. Zhang, H. Chen, K. Liang, and X. Chen, "A novel extended Kalman filter with support vector machine based method for the automatic diagnosis and segmentation of brain tumors," *Comput. Methods Programs Biomed.*, vol. 200, p. 105797, 2021, doi: 10.1016/j.cmpb.2020.105797.

20 M. Shahajad, D. Gambhir, and R. Gandhi, "Features

extraction for classification of brain tumor MRI images using support vector machine," *Proc. Conflu. 2021 11th Int. Conf. Cloud Comput. Data Sci. Eng.*, pp. 767–772, 2021, doi: 10.1109/Confluence51648.2021.9377111.

21 M. S. Drew and N. Nr, "Retinex," pp. 73–79.

22 A. K. Jain, M. N. Murty, and P. J. Flynn, "Data clustering: A review," *ACM Comput. Surv.*, vol. 31, no. 3, pp. 264–323, 1999, doi: 10.1145/331499.331504.

23 A. Chaudhary and V. Bhattacharjee, "An efficient method for brain tumor detection and categorization using MRI images by K-means clustering DWT," *Int. J. Inf. Technol.*, vol. 12, no. 1, pp. 141–148, 2020, doi: 10.1007/s41870-018-0255-4.

24 A. Gokulalakshmi, S. Karthik, N. Karthikeyan, and M. S. Kavitha, "ICM-BTD: improved classification model for brain tumor diagnosis using discrete wavelet transform-based feature extraction and SVM classifier," *Soft Comput.*, vol. 24, no. 24, pp. 18599–18609, 2020, doi: 10.1007/s00500-020-05096-z.

25 Y. Liu, A. Singleton, and D. Arribas-Bel, "A Principal Component Analysis (PCA)-based framework for automated variable selection in geodemographic classification," *Geo-Spatial Inf. Sci.*, vol. 22, no. 4, pp. 251–264, 2019, doi: 10.1080/10095020.2019.1621549.

26 K. Yepuganti, S. Saladi, and C. V. Narasimhulu, "Segmentation of tumor using PCA based modified fuzzy C means algorithms on MR brain images," *Int. J. Imaging Syst. Technol.*, vol. 30, no. 4, pp. 1337–1345, 2020, doi: 10.1002/ima.22451.

27 J. Amin, M. Sharif, M. Yasmin, and S. L. Fernandes, "A distinctive approach in brain tumor detection and classification using MRI," *Pattern Recognit. Lett.*, vol. 139, pp. 118–127, 2020, doi: 10.1016/j.patrec.2017.10.036.

28 H. Fabelo et al., "Spatio-spectral classification of hyperspectral images for brain cancer detection during surgical operations," *PLoS One*, vol. 13, no. 3, pp. 1–27, 2018, doi: 10.1371/journal.pone.0193721.